Hydrol. Earth Syst. Sci. Discuss., 10, 14675–14704, 2013
www.hydrol-earth-syst-sci-discuss.net/10/14675/2013/
doi:10.5194/hessd-10-14675-2013

Hydrology and Earth System Sciences
Discussions
Open Access

Development of streamflow drought severity- and magnitude-duration-frequency curves using the threshold level method

J. H. Sung[1], **E.-S. Chung**[2], **and K. S. Lee**[3]

[1]Ministry of Land, Infrastructure and Transport, Yeongsan Flood Control Office, Gwangju, Republic of Korea
[2]Department of Civil Engineering, Seoul National University of Science and Technology, Seoul, 139-743, Republic of Korea
[3]Department of Civil Engineering, Seoul National University, Seoul, Republic of Korea

Received: 5 October 2013 – Accepted: 14 November 2013 – Published: 3 December 2013

Correspondence to: E.-S. Chung (eschung@seoultech.ac.kr)

Published by Copernicus Publications on behalf of the European Geosciences Union.

Abstract

This study developed a comprehensive method to quantify streamflow drought severity and magnitude based on a traditional frequency analysis. Two types of curve were developed: the streamflow drought severity-duration-frequency (SDF) curve and the streamflow drought magnitude-duration-frequency (MDF) curve (e.g., a rainfall intensity-duration-frequency curve). Severity was represented as the total water deficit volume for the specific drought duration, and magnitude was defined as the daily average water deficit. The variable threshold level method was introduced to set the target instream flow requirement, which can significantly affect the streamflow drought severity and magnitude. The four threshold levels utilized were fixed, monthly, daily, and desired yield for water use. The threshold levels for the desired yield differed considerably from the other levels and represented more realistic conditions because real water demands were considered. The streamflow drought severities and magnitudes from the four threshold methods could be derived at any frequency and duration from the generated SDF and MDF curves. These SDF and MDF curves are useful in designing water resources systems for streamflow drought and water supply management.

1 Introduction

Drought is a recurring regional multi-dimensional phenomenon affecting wide areas and large numbers of people. Droughts have dramatically increased in number and intensity over the last few decades (ComEC, 2007). In addition, the demand for water has significantly increased due to population growth and agricultural, energy, and industrial sector expansion; water scarcities have occurred almost every year in many parts of the world (Mishra and Singh, 2011). Thus, drought risk analysis has become more important but is complicated by the lack of a precise drought definition and characteristics.

HESSD
10, 14675–14704, 2013

Drought implies a period of time when the supply of water cannot meet its typical demand. Rainfall deficiencies of sufficient magnitude over prolonged durations and subsequent reductions in streamflow intervene with the normal agricultural and economic activities of a region, leading to a decrease in agriculture production and in turn affecting everyday life. Dracup et al. (1980) defined drought as follows: (1) nature of water deficit (e.g., precipitation, soil moisture, or streamflow); (2) basic time unit of data (e.g., month, season, or year); (3) threshold for distinguishing low flows from high flows while considering the mean, median, mode, or any other derived threshold; and (4) regionalization and/or standardization. Based on these definitions, various indices have been proposed over the years to identify, characterize, and quantify the attributes of various drought components, such as meteorological, hydrological, and agricultural factors. That is, recent studies have focused on such multi-faceted drought characteristics using various indices (Palmer, 1965; Rossi et al., 1992; McKee et al., 1993; Byun and Wilhite, 1999; Tsakiris et al., 2007; Pandey et al., 2008a, b; 2010; Nalbantis and Tsakiris, 2009; Wang et al., 2011; Tabari et al., 2013).

However, drought is closely related to the deficiency of available water that negatively affects general crops, causes temporary water scarcity for human/livestock consumption, and influences economic renewable resources. Tallaksen and van Lanen (2004) defined drought as a "sustained and regionally extensive occurrence of below average water availability". Therefore, threshold level approaches to define the duration, severity, and magnitude of a drought event while considering the daily, monthly, seasonal, and annual natural runoff variations have been widely applied for drought analyses (Yevjevich, 1967; Sen, 1980; Dracup et al., 1980; Kjeldsen et al., 2000; Hisdal and Tallaksen, 2003; Wu et al., 2007; Pandey et al., 2008a; Tigkas et al., 2012; van Huijgevoort, 2012). These approaches provide an analytical interpretation of the expected availability of river flow; a drought occurs when the streamflow falls below the threshold level. This level is frequently taken as a certain percentile flow and is assumed to be steady during the considered month, season, or year. Kjeldsen et al. (2000)

HESSD
10, 14675–14704, 2013

extended the steady threshold concept to the variable method, employing monthly and daily streamflows.

Based on the reported drought definitions and threshold level approaches, this study developed a comprehensive concept to quantify the streamflow drought severity and magnitude using a traditional frequency analysis. Two streamflow drought severity-duration-frequency (SDF) and magnitude-duration-frequency (MDF) curves with three variable and one fixed threshold levels were proposed using traditional frequency analyses. This methodology was applied to the Seomjin River basin in South Korea.

2 Methodology

2.1 Procedure

This study consists of five steps, as shown in Fig. 1. Step 1 is to determine the threshold levels for fixed, monthly, daily, and monthly desired yield for water use. Step 2 is to calculate the total water deficit volumes (or severity), durations, and daily average water deficits (or magnitude) for all drought events at the four threshold levels. Step 3 is to identify the best-fitted probability distribution functions of annual maximum SDF and MDF using *L*-moment ratio diagrams. Step 4 is to develop four SDF and MDF curves with four threshold levels using the selected probability distribution. Step 5 is to compare all SDFs and MDFs with the four threshold levels.

2.2 Streamflow drought severity and magnitude

In temperate regions where the runoff values are typically larger than zero, the most widely used method to estimate a hydrological drought is the threshold level approach (Yevjevich, 1967; Fleig et al., 2006; Tallaksen et al., 2009; Van Loon and Van Lanen, 2012). The threshold level method has the following advantages over other SPI (Standardized Precipitation Index) and PDSI (Palmer Drought Severity Index): (1) no a priori knowledge of probability distributions is required and (2) drought characteristics, such as frequency, duration, and severity, are directly produced if the threshold is set by sectors impacted by the drought.

A sequence of drought events can be obtained using the streamflow and variable threshold level method. Each drought event is characterized by its duration, D_i, deficit volume (or severity), S_i, and time of occurrence, T_i, as shown by the definition sketch in Fig. 2. With a prolonged dry period, the long drought spell is divided into a number of minor drought events. Because these droughts are mutually dependent, Tallaksen et al. (1997) proposed that the independent sequence of drought events must be described using some types of pooling, as described below.

If the "inter-event" time t_i between two droughts of duration d_i and d_{i+1} and severity s_i and s_{i+1}, respectively, are less than the predefined critical duration t_c, and the ratio between the inter-event excess volume z_c, the mutually dependent drought events were pooled to form a drought event as (Zelenhasic and Salvai, 1987; Tallaksen et al., 1997)

$$d_\mathrm{pool} = d_i + d_{i+1} + t_\mathrm{c},$$
$$s_\mathrm{pool} = s_i + s_{i+1} - z_\mathrm{c} \tag{1}$$

This study assumed t_c = 3 days and z_c = 10 % of d_i or d_{i+1} for simplicity. This numbers should be studied later in more detail.

To further describe the degree of hardship due to a drought event, the daily average water deficit magnitude of independent drought events is proposed and defined as follows:

$$m_i = \frac{s_i}{d_i}. \tag{2}$$

Therefore, this study defined severity and magnitude as two different meanings, total water deficit magnitude and daily average water deficit magnitude, for a specific duration.

HESSD
10, 14675–14704, 2013

2.3 Threshold selection

The threshold choice is influenced by the study objective and region and available data. In general, a percentile from the flow duration curve (FDC) can be used as the threshold. Relatively low thresholds in the range of Q_{70} to Q_{95} are often used for perennial rivers (Kjeldsen et al., 2000). This study selected Q_{70} for the fixed threshold considering the Korean hydrologic condition, namely, a monsoon climate.

A constant threshold from the FDC based on the entire record period is used in Fig. 3 (top). The threshold can also be fixed using only the flow data from the relevant season studied if seasonal deficits are studied separately. Figure 3 presents two seasonal thresholds for summer and winter seasons using variable monthly and daily threshold approaches. This study used a fixed threshold based on the water demand to the reservoir.

2.4 Probability distribution function

L-moment diagrams of various goodness-of-fit techniques were used to evaluate the best probability distribution function for datasets in several recent studies (Hosking, 1990; Chowdhury et al., 1991; Vogel and Fennessey, 1993; Hosking and Wallis, 1997). The L-moment ratio diagram is a graph where the sample L-moment ratios, L-skewness (τ_3), and L-kurtosis (τ_4) are plotted as a scatterplot and compared with the theoretical L-moment ratio curves of candidate distributions. L-moment ratio diagrams have been suggested as a useful graphical tool for discriminating amongst candidate distributions for a dataset (Hosking and Wallis, 1997), Two representations used to assist in the selection of statistical distributions are the sample average and line of best fit, which can be plotted on the same graph to facilitate selecting the best-fit distribution.

When plotting an L-moment ratio diagram, the relationship between the parameters and L-moment ratios τ_3 and τ_4 for several distributions are required. In the case of a GEV distribution, the three-parameter GEV distribution described by Stedinger et al. (1993) has the following probability density function (PDF) and cumulative distribution function (CDF):

$$f(x) = \frac{1}{\alpha}\left(1-\frac{\kappa}{\alpha}(x-\xi)\right)^{1/\kappa-1}\cdot\exp\left(-\left(1-\frac{\kappa}{\alpha}(x-\xi)\right)^{1/\kappa}\right) \qquad \kappa \neq 0, \tag{3a}$$

$$f(x) = \frac{1}{\alpha}\exp\left(-\frac{x-\xi}{\alpha}-\exp\left(-\frac{x-\xi}{\alpha}\right)\right) \qquad \kappa = 0, \tag{3b}$$

$$F(x) = \exp\left(-\left(1-\frac{\kappa}{\alpha}(x-\xi)\right)^{1/\kappa}\right) \qquad \kappa \neq 0, \tag{4a}$$

$$F(x) = \exp\left(-\exp\left(-\frac{x-\xi}{\alpha}\right)\right) \qquad \kappa = 0, \tag{4b}$$

where $\xi+\alpha/\kappa \leq x \leq \infty$ for $\kappa < 0$; $-\infty \leq x \leq \infty$ for $\kappa = 0$; and $-\infty \leq x \leq \xi+\alpha/\kappa$ for $\kappa > 0$. Here, ξ is a location, α is a scale, and κ is a shape parameter. For $\kappa = 0$, the GEV distribution reduces to the classic Gumbel (EV1) distribution with $\tau_3 = 0.17$. Hosking and Wallis (1997) provided more detailed information regarding the GEV distribution. The relationship between the parameters and τ_3 and τ_4 for the shape parameter's GEV distribution can be obtained as follows (Hosking and Wallis, 1997):

$$\tau_3 = \frac{2(1-3^{-\kappa})}{(1-2^{-\kappa})} - 3, \tag{5a}$$

$$\tau_4 = \frac{5(1-4^{-\kappa})-10(1-3^{-\kappa})+6(1-2^{-\kappa})}{(1-2^{-\kappa})}. \tag{5b}$$

3 Study region

The Seomjin River basin is located in southwestern Korea (Fig. 4). The area and total length of the Seomjin River are approximately 4911.9 km^2 and 212.3 km, respectively.

HESSD
10, 14675–14704, 2013

The altitude range is rather large, spanning from approximately 0 to 1646 m (Fig. 4). The climate of South Korea is characterized by extreme seasonal variations. Winter is cold and dry under the dominant influence of the Siberian air mass, whereas the summer is hot and humid with frequent heavy rainfall associated with the East Asian monsoon. In the Seomjin River basin, the measured precipitation is mainly concentrated in summer, and the measured mean annual precipitation varies from < 1350 mm yr^{-1} (in the north region) to > 1600 mm yr^{-1} (in the southeastern region) during the 1975–2012 observation period. In general, approximately 60 % of the annual precipitation occurs during the wet season (July through September) in South Korea. This extreme seasonality in the precipitation causes periodic shortages of water during the dry season (October through March) and flood damage during the wet season.

The administrative districts where the basin is located cover three provinces, four cities, and 11 countries (Namwon City, Jinan County, Imsil Country, and Sunchang County in the Northern Jeolla Province; Suncheon City, Gwangyang City, Damyang County, Gokseong County, Gurye County, Hwasun County, Boseong County, and Jangheung County in the Southern Jeolla Province; and Handing County in the Southern Gyungsang Province). Influx rates into the basin by province are 47 % (Southern Jeolla Province), 44 % (the Northern Jeolla Province), and 9 % (Southern Gyeongsang Province), and a total of 129 322 households and 321 104 residents live in these areas.

The land use consists of arable land (876.29 km^2), forest land (3400.61 km^2), building sites (67.12 km^2), and other land uses (567.86 km^2). Additionally, 69.2 % of the entire basin area (4,911.89 km^2) is forest land. Major droughts occurred in the Southern Jeolla Province from 1967 to 1968 and from 1994 to 1995. The Seomjin River basin had < 1000 mm of precipitation on average in 1977, 1988, 1994, and 2008. Among these years, the annual precipitation in 1988 was only 782.7 mm (56.5 %) of the annual average of 1385.5 mm from 1967 to 2008, representing a serious drought. According to the "River Survey Report (K-water, 1992)", a drought in Seomjin river basin occurs approximately every 10 yr.

HESSD
10, 14675–14704, 2013

4 Results

4.1 Determination of the threshold levels

This study used four threshold levels, as described in Fig. 3. The calculated thresholds are presented in Fig. 5, and the specific values are listed in Table 1. The annual average threshold levels were 8.30, 11.80, 17.90, and 13.81 $m^3 s^{-1}$ for the fixed, monthly, daily, and desired yields, respectively. The daily threshold levels were highly fluctuating because of the natural streamflow variations for the antecedent 365 days and were the largest of the four threshold levels because a summer period was considered. The fixed threshold level was larger than the minimum levels for the daily, monthly, and desired yields. This phenomenon occurred during the winter in Korea, and as a result, both the water demand and natural runoff during the winter were quite small. However, the thresholds levels for the daily, monthly, and desired yields during the summer were much higher than during the other seasons.

The threshold levels for the desired yield during May were much larger than the levels for the other thresholds because the agricultural water demand was the highest in this season. However, the levels for the desired yield during May were smaller than the other threshold levels.

4.2 Calculations of severity and magnitude

The durations, total drought volumes, and magnitudes of all streamflow drought events were calculated based on the streamflow drought concept and threshold levels. The summarized values are listed in Table 2. The maximum durations from the desired yield threshold approach were considerably higher than those from the other thresholds because the desired yields were highest during May and June due to agricultural water use. However, the maximum streamflow drought severities and magnitudes of the daily and monthly threshold approaches were higher than those from the other thresholds. The daily threshold displays the highest number of drought events because the impacts of natural and artificial factors, such as climate variables, water use, land use change, and other physical variations, were reflected in this threshold.

The analysis using the fixed threshold level indicated that 146 streamflow droughts occurred from 1975 to 2012. The five largest drought durations, volumes, and magnitudes are listed in Table 3. The longest drought lasted for 102 days (28 September 1988–7 October 1989) and it generated the largest total drought volume. The total drought volume exhibited a trend similar to that of the duration, because the volumes became large when the duration was longer. However, the magnitude trend was completely different from the previous two results. The drought with the largest magnitude occurred on 23 September 1987. Three of the top five largest drought magnitudes had short durations of less than seven days. Therefore, the severity and magnitude decreased with increasing duration, such as rainfall intensity-duration-frequency (IDF). Similar patterns were observed in the results from the monthly and daily threshold approaches.

The duration and magnitude relationships were investigated using the remaining three threshold methods, and the results are presented in Fig. 6. The annual maxima values of duration, total volume, and magnitude were derived using the above results. The durations from the four methods exhibited slight differences, whereas the total volumes and magnitudes exhibited large differences. To confirm the consistency of our approach, the correlation coefficients among the four results were calculated and are presented in Table 4. The same trend was observed in the fixed, monthly, and daily threshold levels. However, the durations, total volumes, and magnitudes from the desired yield threshold level were completely different. That is, the drought identification techniques based on real precipitation and natural streamflows did not reflect the drought concept in terms of water supply and water use. Therefore, two-way approaches should be included for specific drought identification and analysis.

4.3 Identification of the probability distribution function

The L-moment diagrams of various goodness-of-fit techniques were used to evaluate the best probability distribution function for datasets in several recent studies. The L-moment ratio diagram is a graph in which the sample L-moment ratios, L-skewness, and L-kurtosis are plotted as a scatterplot and compared with the theoretical L-moment ratio curves of candidate distributions. L-moment ratio diagrams have been suggested to be a useful graphical tool for discriminating amongst candidate distributions for a dataset (Hosking and Wallis, 1997). Two representations used to assist in selecting statistical distributions are the sample average and line of best fit, which can be plotted on the same graph to facilitate the selection of the best-fit distribution. To develop an SDI MDF curve, the proper probability distribution function should be determined based on the statistical results, as described in Sect. 2.4.

The L-moment ratio diagrams were derived for the four threshold approaches and are displayed in Fig. 7. Of the distribution models tested, only the Pearson Type 3 (PT3), Generalized Normal (GNO), and Generalized Extreme Value (GEV) distributions appeared consistent with their datasets, and of those three distributions, fewer than half of the observations approached the GEV line. Thus, the GEV distribution was selected as a representative distribution. In Fig. 7, the red, blue, black, and grey colored dots denote the durations, total volumes (severities), magnitudes, and maximum deficit volumes, respectively.

4.4 Development of the SDF and MDF curves

SDF and MDF curves were developed using the derived probability distribution functions, as shown in Figs. 8 and 9, respectively. For these plots, two, five, 10, 20, 50, and 100 yr-frequency magnitudes were calculated at 10, 20, 30, and 40 day durations. SDF and MDF described two types of relationships: (1) streamflow drought total water deficit volume and (severity)-duration-frequency and (2) streamflow drought daily average water deficit and (magnitude)-duration-frequency. The total water deficit volume increased with increasing duration, whereas the average daily water deficit decreased with increasing duration. In the SDF curve, the severity from the fixed threshold varied considerably, whereas the severity from the desired yield threshold exhibited relatively small differences. In contrast, in the MDF curve, the variations exhibited the opposite trend. The magnitudes from the desired yield threshold varied considerably, whereas the magnitudes from the fixed threshold exhibited relatively small variations.

The total and average daily water deficits increased with increasing frequencies. In addition, the severity and magnitude decreased as the duration increased. SDF and MDF curves can be very useful for developing appropriate water resources management strategies with respect to specific streamflow drought severities and magnitudes.

Four threshold level approaches were used to quantify streamflow drought severity and magnitude. Table 5 compares all of the severities and magnitudes of each frequency and duration. In the case of SDF, monthly and daily threshold levels produced the largest water deficit volumes for all durations. The fixed threshold level exhibited a slightly smaller water deficit. In contrast, the water supply demand threshold exhibited a very dynamic and wide-ranging deficit volume; from 10^2 to 10^8 m^3 depending on its duration. In the case of MDF, the fixed threshold level approach exhibited a very small water deficit, whereas the daily threshold level had the highest maximum daily water deficit. However, these values were quite different because the four threshold level approaches defined the streamflow drought differently.

5 Conclusions

This study developed a novel concept to describe the characteristics of streamflow droughts using frequency analyses. SDF and MDF curves for streamflow drought were developed to quantify a specific volume according to a specific duration and frequency. This study used severity and magnitude, which represented the total water deficit and average daily water deficit, respectively, for the specific durations. Using the L-moment diagram method, the GEV was selected for the best-fit probability distribution. As a result, SDF and MDF curves were derived to evaluate two relationships: (1) streamflow drought total water deficit volume-duration-frequency and (2) streamflow drought average daily water deficit-duration-frequency. The total water deficit volume increased with increasing duration, whereas the average daily water deficit decreased with increasing duration. The total and average daily water deficits increased with increasing frequencies. However, these values were quite different because the four threshold level approaches defined the streamflow drought differently. SDF and MDF curves can be very useful for developing appropriate water resources management strategies with respect to specific streamflow drought magnitudes.

This study can be applied to various hydrologic analyses and water resources management systems, such as desired yield and dam safe yield. In addition, our SDI MDF method will be extended to conduct regional frequency analyses, which can estimate SDI magnitudes at ungagged sites.

Acknowledgements. This study was supported by the funding from the Basic Science Research Program of the National Research Foundation of Korea (2010-0010609). This research was supported by a grant (11-TI-C06) from Advanced Water Management Research Program funded by Ministry of Land, Infrastructure and Transport of Korean government.

References

Byun, H.-R. and Wilhite, D. A.: Objective quantification of drought severity and duration, J. Climate, 12, 747–756, 1999.

Chowdhury, J. U., Stedinger, J. R., and Lu, L.-H.: Goodness-of-fit tests for regional generalized extreme value flood distributions, Water Resour. Res., 27, 1765–1776, 1991.

ComEC (Commission of the European Communities): Communication from the commission to the European parliament and the council: addressing the challenge of water scarcity and droughts in the European Union, Commission of the European Communities, Brussels, 2007.

Dracup, J. A., Lee, K. S., and Paulson Jr., E. G.: On the statistical characteristics of drought events, Water Resour. Res., 16, 289–296, 1980.
Fleig, A. K., Tallaksen, L. M., Hisdal, H., and Demuth, S.: A global evaluation of streamflow drought characteristics, Hydrol. Earth Syst. Sci., 10, 535–552, doi:10.5194/hess-10-535-2006, 2006.
Hisdal, H. and Tallaksen, L. M.: Estimation of regional meteorological and hydrological drought characteristics: a case study for Denmark, J. Hydrol., 281, 230–247, 2003.
Hosking, J. R. M.: *L*-moments: analysis and estimation of distributions using linear combinations of order statistics, J. R. Stat. Soc. B, 52, 105–124, 1990.
Hosking, J. R. M. and Wallis, J. R.: Regional Frequency Analysis: an Approach Based on *L*-Moments, Cambridge Univ. Press, New York, 1997.
Kjeldsen, T. R., Lundorf, A., and Dan, R.: Use of two component exponential distribution in partial duration modeling of hydrological droughts in Zimbabwean rivers, Hydrolog. Sci. J., 45, 285–298, 2000.
McKee, T. B., Doesken, N. J., and Kleist, J.: The relationship of drought frequency and duration to time scales, Proc. 8th Conf. Appl. Climatol., American Meteor. Soc., Boston, 179–184, 17–22 January, 1993.
Mishra, A. K. and Singh, V. P.: Drought modeling: a review, J. Hydrol., 403, 157–175, 2011.
Nalbantis, I. and Tsakiris, G.: Assessment of hydrological drought revisited, Water Resour. Manag., 23, 881–897, 2009.
Palmer, W. C.: Meteorological drought, Research Paper No. 45, US Department of Commerce Weather Bureau, Washington DC, 1965.
Pandey, R. P., Mishra, S. K., Singh, R., and Ramasastri, K. S.: Streamflow drought severity analysis of Betwa river system (India), Water Resour. Manag., 22, 1127–1141, 2008a.
Pandey, R. P., Sharma, K. D., Mishra, S. K., Singh, R., and Galkate, R. V.: Assessing streamflow drought severity using ephemeral streamflow data, Int. J. Ecol. Econ. Stat., 11, 77–89, 2008b.
Pandey, R. P., Pandey, A., Galkate, R. V., Byun, H.-R., and Mal, B. C.: Integrating hydro-meteorological and physiographic factors for assessment of vulnerability to drought, Water Resour. Manag., 24, 4199–4217, 2010.
Rossi, G., Benedini, M., Tsakins, G., and Giakoumakis, S.: On regional drought estimation and analysis, Water Resour. Manag., 6, 249–277, 1992.

Sen, Z.: Statistical analysis of hydrologic critical droughts, J. Hydraul. Div. ASCE, 106, 99–115, 1980.
Stedinger, J. R., Vogel, R. M., and Foufoula-Georgiou, E.: Frequency analysis of extreme events, chapter 18, in: Handbook of Hydrology, edited by: Maidment, D., McGraw-Hill, Inc., New York, 17–19, 1993.
Tabari, H., Nikbakht, J., and Talaee, P. H.: Hydrological drought assessment in Northwestern Iran based on streamflow drought index (SDI), Water Resour. Manag., 27, 137–151, 2013.
Tallaksen, L. M. and van Lanen, H. A. J.: Hydrological Drought: Processes and Estimation Methods for Streamflow and Groundwater, Developments in Water Science, Vol. 48, Elsevier Science B. V., 2004.
Tallaksen, L. M., Madsen, H., and Clusen, B.: On the definition and modeling of streamflow drought duration and deficit volume, Hydrolog. Sci. J., 42, 15–33, 1997.
Tallaksen, L. M., Hisdal, H., and van Lanen, H. A. J.: Space-time modelling of catchment scale drought characteristics, J. Hydrol., 375, 363–372, 2009.
Tigkas, D., Vangelis, H., and Tsakiris, G.: Drought and climatic change impact on streamflow in small watersheds, Sci. Total. Environ., 440, 33–41, 2012.
Tsakiris, G. and Pangalou, D.: Regional drought assessment based on Reconnaissance Drought Index (RDI), Water Resour. Manag., 21, 821–833, 2007.
van Huijgevoort, M. H. J., Hazenberg, P., van Lanen, H. A. J., and Uijlenhoet, R.: A generic method for hydrological drought identification across different climate regions, Hydrol. Earth Syst. Sci., 16, 2437–2451, doi:10.5194/hess-16-2437-2012, 2012.
Van Loon, A. F. and Van Lanen, H. A. J.: A process-based typology of hydrological drought, Hydrol. Earth Syst. Sci., 16, 1915–1946, doi:10.5194/hess-16-1915-2012, 2012.
Vogel, R. M. and Fennessey, N. M.: *L*-moment diagrams should replace product moment diagrams, Water Resour. Res., 29, 1745–1752, 1993.
Wang, A., Lettenmaier, D. P., and Sheffield, J.: Soil moisture drought in China, 1950–2006, J. Climate, 24, 3257–3271, 2011.
World Meteorological Organization: Manual on Low-flow Estimation and Prediction, Operational Hydrology Report No. 50, 2008.
Wu, J., Soh, L. K., Samal, A., and Chen, X. H.: Trend analysis of streamflow drought events in Nebraska, Water Resour. Manag., 22, 145–164, 2007.

HESSD
10, 14675–14704, 2013

Threshold level method

J. H. Sung et al.

Yevjevich, V.: An objective approach to definition and investigation of continental hydrological droughts, Hydrology Paper No. 23, Colorado State University, Fort Collins, Colorado, USA, 1967.
Zelenhasic, E. and Salvai, A.: A method of streamflow drought analysis, Water Resour. Res., 23, 156–168, 1987.

HESSD
10, 14675–14704, 2013

Table 1. Monthly averaged of four threshold levels.

	Threshold level [$m^3 s^{-1}$]			
	Fixed	Monthly	Daily	Desired yield
Jan	8.300	3.800	3.918	5.420
Feb	8.300	5.562	7.291	4.392
Mar	8.300	10.100	9.947	2.281
Apr	8.300	10.017	12.784	4.238
May	8.300	7.632	9.906	9.245
Jun	8.300	9.590	19.975	39.243
Jul	8.300	38.006	57.472	34.843
Aug	8.300	28.784	50.423	38.645
Sep	8.300	15.877	29.717	15.021
Oct	8.300	3.590	4.150	4.039
Nov	8.300	3.330	3.699	3.992
Dec	8.300	4.200	4.295	3.760

HESSD
10, 14675–14704, 2013

J. H. Sung et al.

Table 2. Summary of four threshold approaches.

Threshold level method	Maximum duration	Maximum Severity (m^3)	Maximum Magnitude ($m^3\,day^{-1}$)	Number of drought event
Fixed	102	148 052 571	2 160 000	146
Monthly	69	486 860 297	21 031 611	244
Daily	49	654 836 708	24 789 394	533
Desired yield	278	291 115 728	2 885 935	256

HESSD
10, 14675–14704, 2013

Table 3. Top five largest drought events to duration, total drought volume and magnitude from fixed threshold approach.

Category	Drought order	Duration	Severity	Magnitude	Start year	month	day
Duration	50	102	148 052 571	1 451 495	1988	Sep	28
	81	68	107 654 400	1 583 152	1995	Nov	4
	35	56	86 930 742	1 552 334	1984	Jan	13
	137	49	38 966 400	795 233	2008	Oct	27
	7	46	82 524 342	1 794 007	1977	Oct	3
Severity	50	102	148 052 571	1 451 495	1988	Sep	28
	81	68	107 654 400	1 583 152	1995	Nov	4
	35	56	86 930 742	1 552 334	1984	Jan	13
	7	46	82 524 342	1 794 007	1977	Oct	3
	48	31	62 862 171	2 027 812	1987	Sep	26
Magnitude	49	1	2 160 000	2 160 000	1987	Nov	23
	56	21	44 755 200	2 131 200	1990	Oct	10
	146	3	6 356 571	2 118 857	2012	Jun	21
	52	4	8 405 486	2 101 371	1989	Aug	7
	53	19	39 793 371	2 094 388	1989	Oct	10

Table 4. Correlations between four threshold approach.

Duration	Fixed	Monthly	Daily	Desired yield
Fixed	1			
Monthly	0.870	1		
Daily	0.888	0.975	1	
Desired yield	0.075	0.200	0.237	1
Total volume	**Fixed**	**Monthly**	**Daily**	**Desired yield**
Fixed	1			
Monthly	0.684	1		
Daily	0.696	0.961	1	
Desired yield	0.139	0.418	0.360	1
Magnitude	**Fixed**	**Monthly**	**Daily**	**Desired yield**
Fixed	1			
Monthly	0.686	1		
Daily	0.666	0.760	1	
Desired yield	0.107	0.272	0.380	1

HESSD
10, 14675–14704, 2013

Table 5. Values of magnitude-duration-frequency at Seomjin River basin.

Method	Duration [day]	Return period [yr] 2 yr	5 yr	10 yr	20 yr	50 yr	100 yr
Fixed	10	9.8	19.9	27.8	36.4	49.5	60.8
	20	4.1	8.3	10.3	11.9	13.4	14.3
	30	2.8	5.6	6.8	7.7	8.5	8.9
	40	1.3	2.6	3.1	3.4	3.6	3.8
Monthly	10	221.2	370.1	518.1	713.6	1077.8	1466.2
	20	111.4	235.4	323.4	412.4	534.9	632.4
	30	39.7	81.6	101.5	116.3	130.7	138.8
	40	29.8	60.0	73.0	81.9	89.8	93.9
Daily	10	412.7	867.9	1591.7	2994.8	7058.8	13 618.7
	20	411.4	803.0	1389.1	2469.7	5422.8	9940.2
	30	385.0	604.8	848.5	1200.5	1925.6	2777.2
	40	341.2	370.1	518.1	713.6	1077.8	1466.2
Desired Yield	10	38.9	57.0	115.8	323.9	1551.7	5299.5
	20	36.7	53.2	86.9	167.2	463.8	1061.3
	30	32.7	51.2	78.0	126.0	253.3	442.3
	40	26.5	39.8	52.7	69.6	100.5	132.9

HESSD
10, 14675–14704, 2013

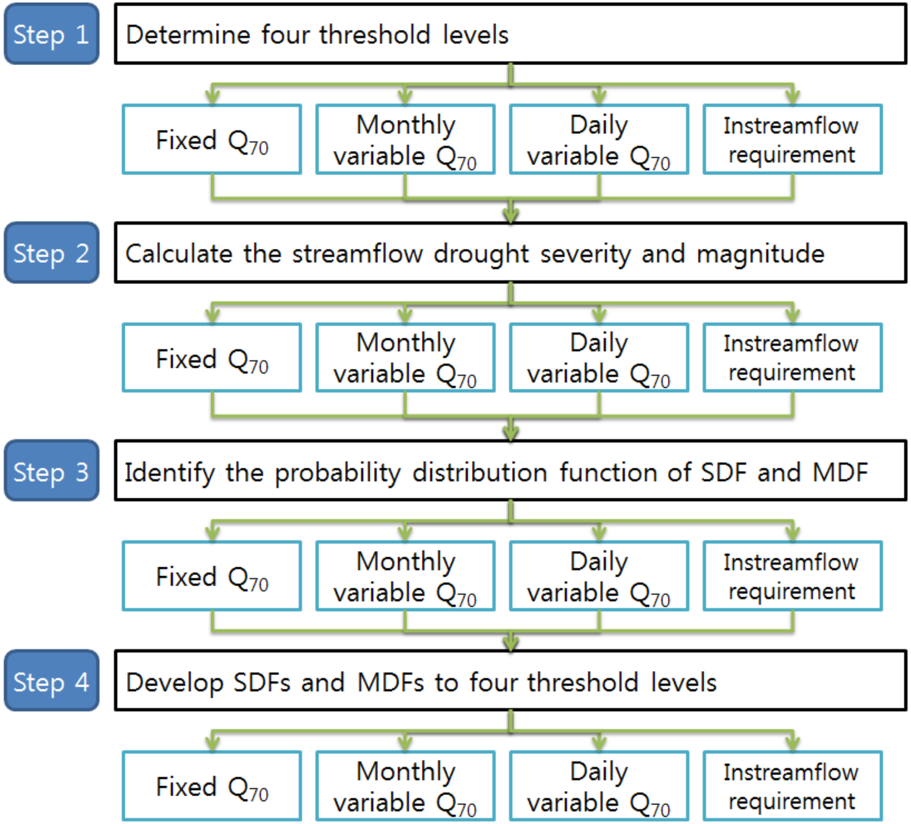

Fig. 1. Procedure of this study.

HESSD
10, 14675–14704, 2013

Threshold level method

J. H. Sung et al.

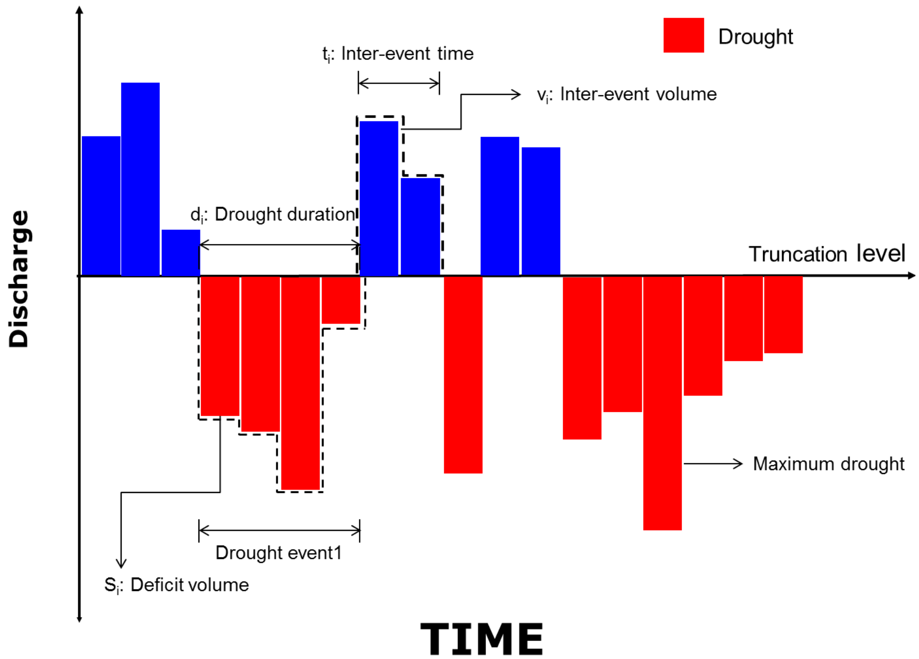

Fig. 2. A definition sketch of general drought events.

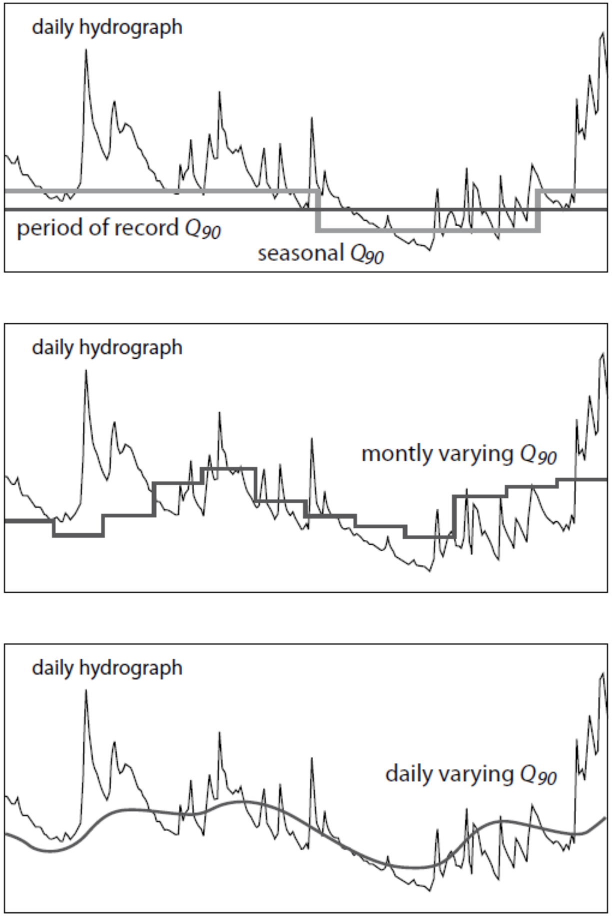

Fig. 3. Examples of threshold levels: fixed (top); monthly varying (middle); daily varying (bottom) (World Meteorological Organization, 2008).

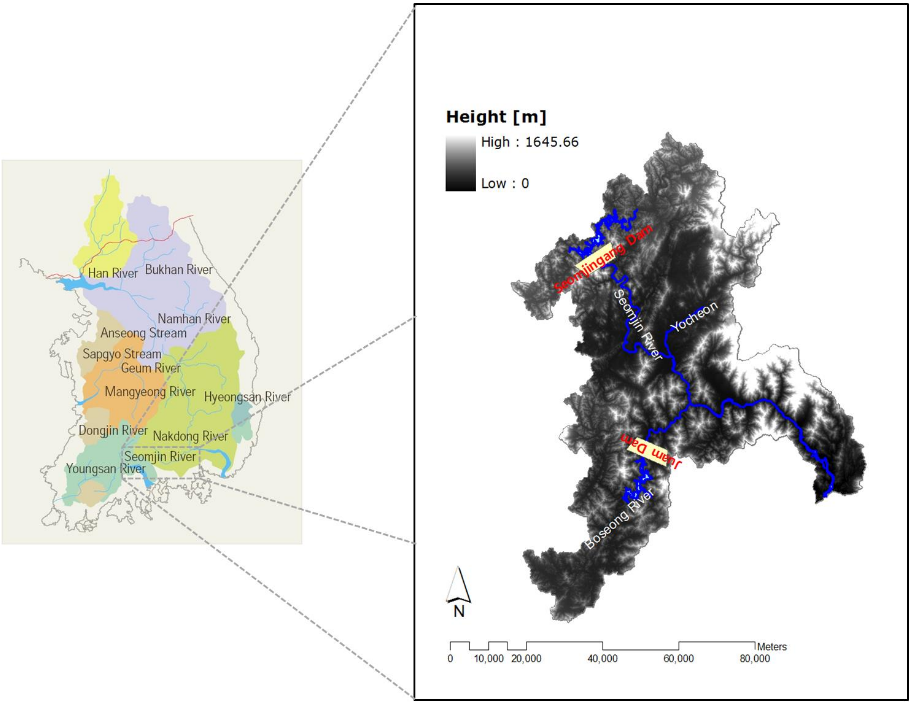

Fig. 4. Location of the selected river basin, including elevation and river.

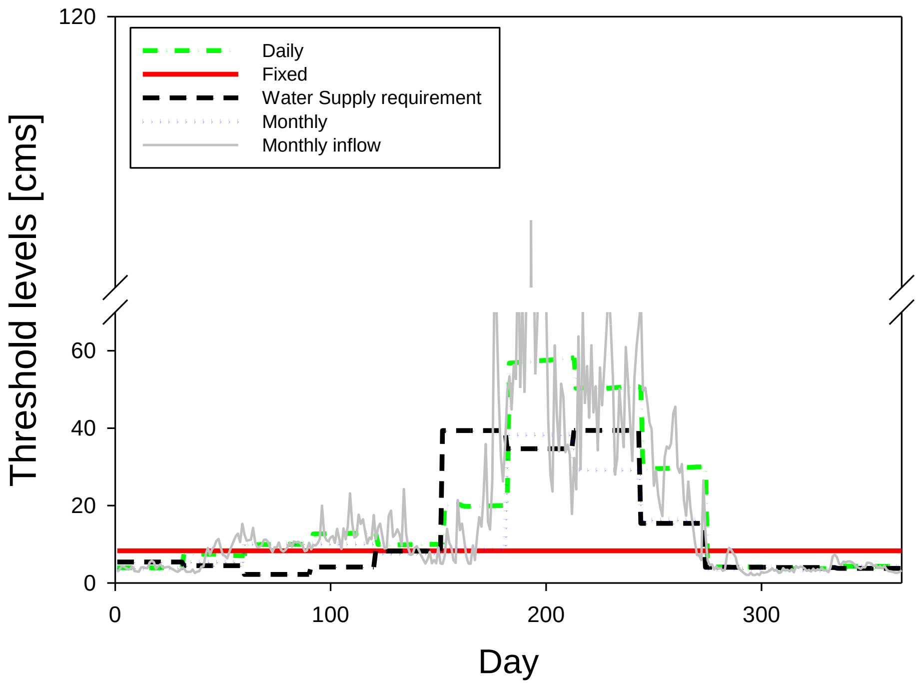

Fig. 5. Yearly averaged threshold levels and monthly inflow.

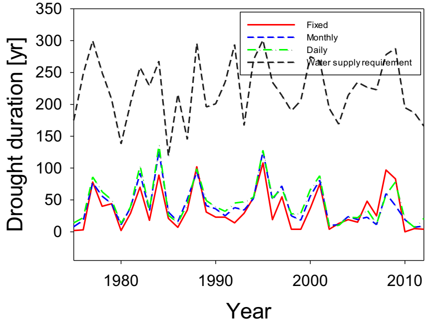

(a) Drought duration

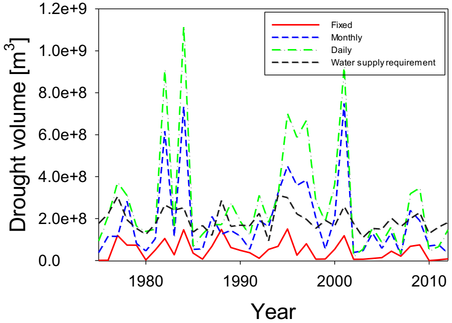

(b) Total water deficit volume (drought severity)

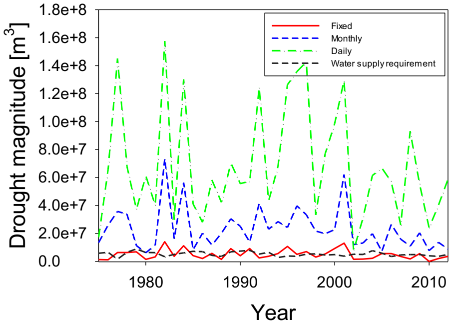

(c) Daily average water deficit (drought magnitude)

Fig. 6. Time series of annual maxima values of duration, severity and magnitude.

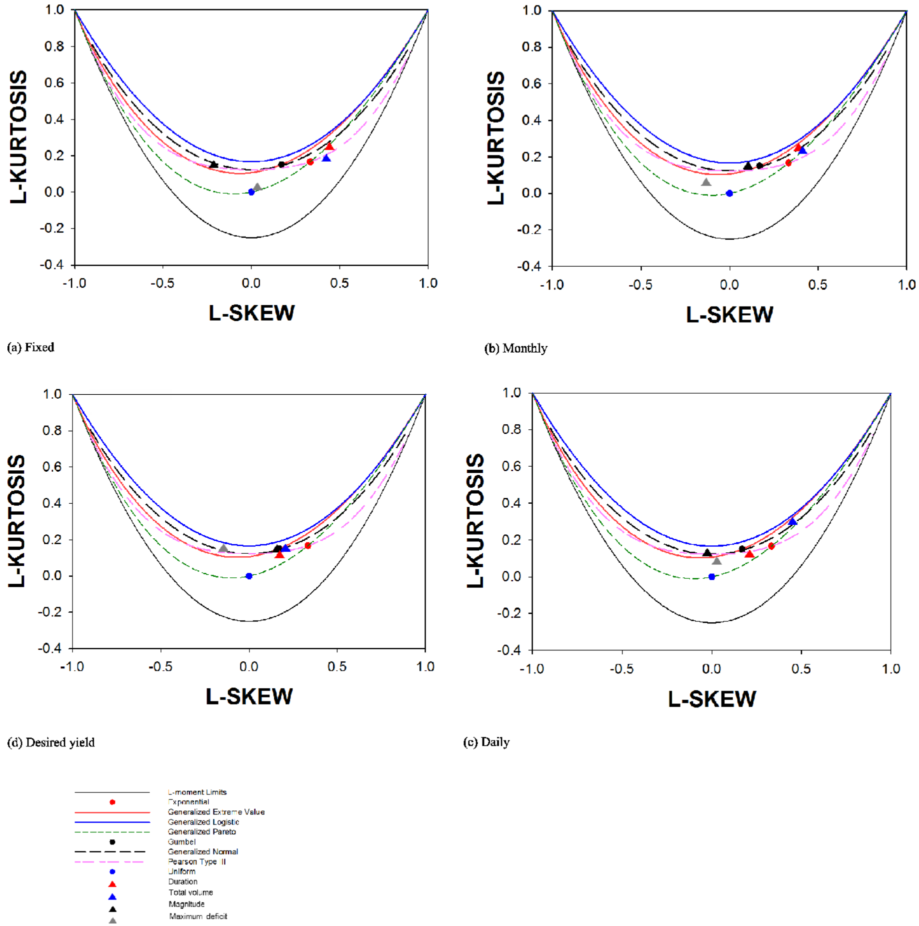

Fig. 7. *L*-moment diagrams for probability distribution identification.

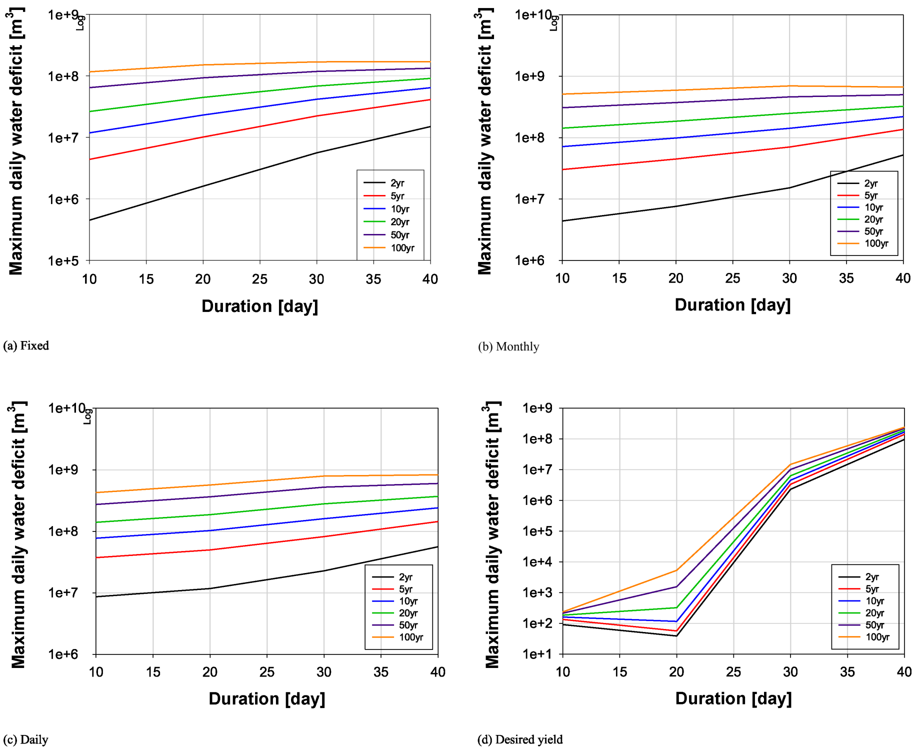

Fig. 8. SDF curves of four threshold approaches in Seomjin river basin.

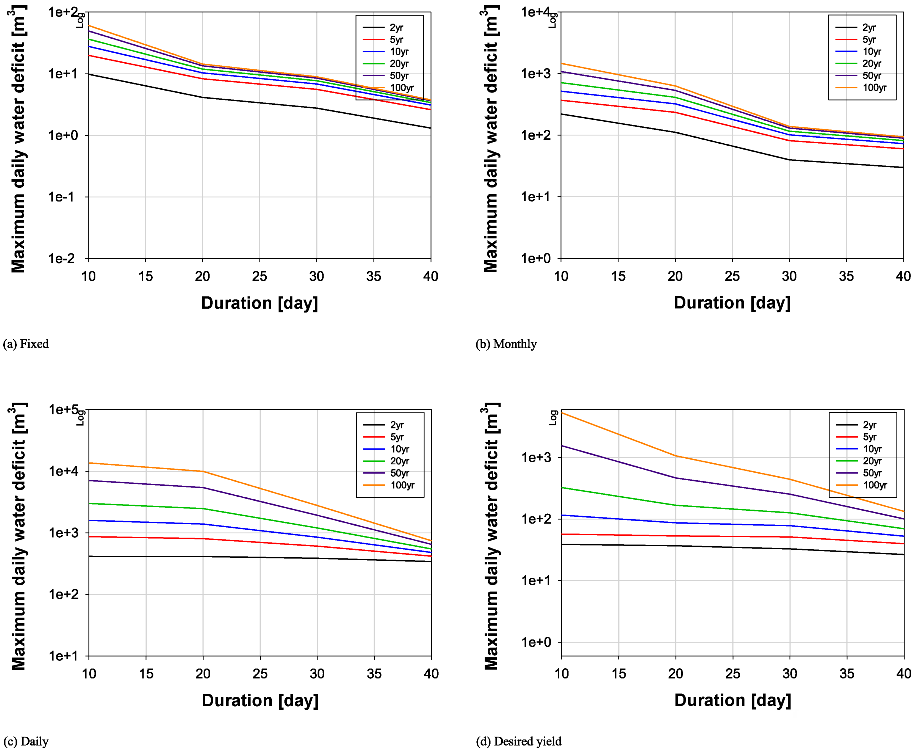

Fig. 9. MDF curves of four threshold level approaches in Seomjin river basin.

HESSD
10, 14675–14704, 2013